JOURNAL OF VIROLOGY, Apr. 1996, p. 2611–2614 Vol. 70, No. 4
0022-538X/96/$04.00+0

Mutational Analysis of the Vaccinia Virus E3 Protein Defines Amino Acid Residues Involved in E3 Binding to Double-Stranded RNA

C. KIONG HO AND STEWART SHUMAN*

Molecular Biology Program, Sloan-Kettering Institute, New York, New York 10021

Received 31 October 1995/Accepted 8 December 1995

Alanine-substitution mutations were targeted to 14 amino acid residues within the double-stranded (ds) RNA binding motif (dsRBM) of the vaccinia virus E3 protein. Substitutions at six positions—Glu-124, Phe-135, Phe-148, Lys-167, Arg-168, and Lys-171—caused significant reductions in dsRNA binding. These six residues are conserved in the two dsRBMs for which structural information is available (*Escherichia coli* RNase III and *Drosophila melanogaster* staufen) and in many other members of the dsRBM protein family. Residues we show to be important for dsRNA binding by vaccinia virus E3 map to the same face of the dsRBM structure and are thus likely to compose part of the RNA binding site.

The vaccinia virus-encoded E3 protein mitigates the antiviral effects of interferon by blocking cellular response pathways dependent on double-stranded (ds) RNA (2, 4, 21). Genetic and biochemical experiments suggest that the biological activity of E3 derives primarily, if not exclusively, from its capacity to bind to dsRNA (4, 5, 6, 21). The C-terminal half of the 190-amino-acid E3 polypeptide is sufficient to bind dsRNA in vitro (4, 22). This region contains a conserved ~65-amino-acid dsRNA binding motif (dsRBM) found in many other proteins that interact with dsRNA (4, 10, 15, 19), including the dsRNA-dependent protein kinase PKR, a key mediator of interferon-induced inhibition of viral protein synthesis and the very enzyme that is targeted by the vaccinia virus E3 protein in vivo.

The dsRBM family is expanding quickly as new members are identified by functional screening of expression libraries (1, 8, 19) or as the dsRBM motif is encountered during genome sequencing efforts (see reference 12 for a recent survey). Multiple repeats of the dsRBM are often present within a single polypeptide. For example, the motif is reiterated five times in *Drosophila melanogaster* staufen (19), three times in human dsRNA-specific adenosine deaminase (dsRAD) (13), and twice in PKR (10). In contrast, vaccinia virus E3 has only one dsRBM, as does *Escherichia coli* RNase III.

To better understand the basis for dsRNA recognition by the vaccinia virus E3 protein, we have examined the effects of single-amino-acid substitutions within the dsRBM on RNA binding. Our work builds on that of Jacobs and coworkers, who defined E3 as the virus-encoded inhibitor of PKR, localized its dsRNA binding function to the C-terminal half, and showed that alterations at selected residues within the conserved dsRBM could affect dsRNA binding by E3 protein translated in vitro (4–6, 21). Our approach has been to study the structure and function of the E3 by using purified recombinant protein. We have expressed full-length 190-amino-acid E3 and a truncated version, E3(100–190), corresponding to the C-terminal dsRNA binding domain (11). Both proteins bind avidly to homopolymeric dsRNA [poly(rI)-poly(rC)] immobilized on agarose; they also bind in solution to a defined 39-mer dsRNA (11).

* Corresponding author. Mailing address: Molecular Biology Program, Sloan-Kettering Institute, 1275 York Ave., New York, NY 10021. Phone: (212) 639-7145. Fax: (212) 717-3623.

Mutagenesis strategy. In the present study, we introduced Ala-substitution mutations at 14 positions in the dsRBM of E3(100–190). The residues mutated included Pro-118 (i.e., mutant P118A), Glu-124, Phe-135, Gly-141, Pro-142, Phe-148, Lys-165, Ser-166, Lys-167, Arg-168, Lys-171, Asn-172, Asn-173, and Lys-176 (denoted by asterisks in Fig. 1). These positions were chosen because they are well conserved in other dsRBMs. For example, the E3 dsRBM strongly resembles the first of three motifs found in dsRAD, an enzyme implicated in posttranscriptional editing of mRNA (13); indeed 12 of 14 of the sites chosen for analysis in E3 are identical or conserved in dsRAD1 (Fig. 1). In each case, the wild-type amino acid of E3 was replaced by alanine. Because alanine substitution eliminates the side chain beyond the β-carbon, usually without perturbing global protein structure, this mutational approach provides an indication of the essentiality of the side chain for protein function.

His-tagged wild-type and Ala-substituted E3(100–190) proteins were expressed under the control of a T7 RNA polymerase promoter in *E. coli* BL21. T7 RNA polymerase was introduced into the cells by infection with phage λCE6 (20). Purification from high-salt extracts of bacterial lysates was achieved by adsorption of the His-tagged proteins to Ni-NTA-agarose and elution with buffer containing 0.5 M imidazole. Sodium dodecyl sulfate-polyacrylamide gel electrophoresis (SDS-PAGE) analysis revealed that each of the affinity-purified protein preparations was homogeneous with respect to the 12-kDa E3(100–190) polypeptide (Fig. 2).

Binding to dsRNA. dsRNA binding was assayed by a variation of the Northwestern blotting technique. In this procedure, the protein is transferred to a membrane, which is then probed with a radiolabeled dsRNA ligand. In conventional applications, the protein sample (which is often impure) is denatured, resolved by SDS-PAGE, transferred from the gel to a membrane, and then renatured on the membrane before being reacted with the ligand. For our purposes, because the E3(100–190) proteins were purified to homogeneity under native conditions, we simply applied the native preparation to a nitrocellulose membrane with a slot blot apparatus and probed with radioactive ligand. To establish the sensitivity and specificity of this assay, serial dilutions of full-sized E3 protein and truncated E3(100–190) were blotted and probed either with 3′-labeled single-stranded poly(rC) or with 3′-labeled poly(rI)-

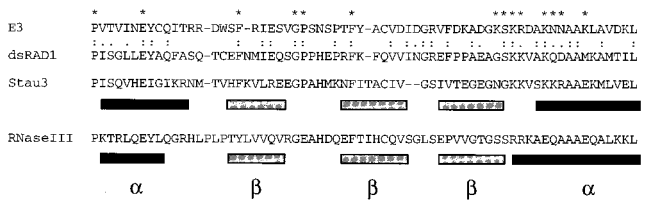

FIG. 1. Amino acids targeted for mutation in the E3 dsRBM. The E3 dsRBM sequence from residues Pro-118 to Leu-182 is displayed in alignment with homologous dsRBMs from human dsRAD1, *Drosophila* staufen (Stau3), and *E. coli* RNase III. The amino acids in the E3 dsRBM that were targeted for mutation in the study are indicated by asterisks above the sequence. The common α-β-β-α secondary structures of the staufen and RNase III dsRBMs (3, 12) are denoted below their sequences.

poly(rC) RNAs. The RNA had been labeled in vitro by transfer of [5′-^{32}P]pCp to the 3′ end of the homopolymer with T4 RNA ligase, as described previously (7, 17). Retention of labeled RNA on the membrane slots was visualized with a PhosphorImager. Full-sized E3 and E3(100–190) bound to dsRNA in buffer containing 50 mM NaCl. Single-stranded poly(C) was not bound by full-length E3 at any level of input protein tested (up to 500 ng). E3(100–190) bound weakly to poly(C) in 50 mM NaCl, but it did not bind single-stranded (ss) RNA at all under the more stringent reaction conditions discussed below. No dsRNA or ssRNA was bound by the equivalent amounts of lysozyme applied to nitrocellulose (Fig. 3). A

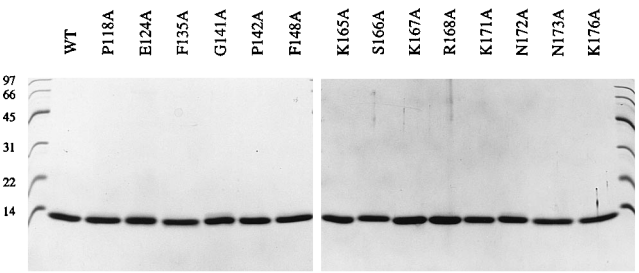

FIG. 2. Recombinant E3(100–190) proteins. A pET-based expression vector was constructed in which the E3 coding sequence from amino acid Ser-100 to C-terminal residue Phe-190 was fused in-frame to a 5′ leader encoding a His tag (Met-Gly-Ser-His-His-His-His-His-His-Ser-Gly-His-Met) (11). Alanine-substitution mutations in E3(100–190) were programmed by synthetic oligonucleotides with the two-stage PCR overlap extension strategy. The presence of the desired mutation was confirmed by dideoxy sequencing. The entire insert of each pET-E3(100–190)-Ala plasmid was sequenced to ensure that no unwanted mutations had been introduced during the PCR and cloning operations. The plasmids were transformed into *E. coli* BL21. Expression of E3(100–190) was induced by infection with bacteriophage λCE6 as described previously (20). Bacteria (from 100-ml cultures) were harvested by centrifugation 4 h postinfection. All subsequent procedures were performed at 4°C. The bacteria were lysed in 5 ml of a mixture containing 50 mM Tris-HCl (pH 7.5), 0.15 M NaCl, 10% sucrose, 0.2 mg of lysozyme per ml, and 0.1% Triton X-100. Insoluble material recovered after centrifugation was resuspended in 1 ml of buffer B (50 mM Tris-HCl [pH 8.0], 10% glycerol, 0.1% Triton X-100) containing 1 M NaCl. Soluble and insoluble fractions were separated by centrifugation. After reextraction of the pellet with 1 ml of 1 M NaCl in buffer B, the supernatant fractions containing soluble E3(100–190) were combined. This material was mixed with 0.2 ml of Ni-NTA-agarose (Qiagen) that had been equilibrated with buffer B containing 1.0 M NaCl. The resin was recovered by centrifugation, and then washed twice with 50 mM imidazole in buffer B containing 0.5 M NaCl. The E3(100–190) protein was eluted with 500 mM imidazole in buffer B containing 0.5 M NaCl. This fraction was dialyzed against buffer B containing 0.5 M NaCl. Protein concentrations were determined with the Bio-Rad dye reagent with bovine serum albumin as the standard. The polypeptide composition of each preparation was analyzed by SDS-PAGE (15% polyacrylamide gel). Three micrograms of protein was applied in each lane, as indicated. Polypeptides were visualized by staining with Coomassie blue dye. Marker proteins were electrophoresed in the extreme left and right lanes; their sizes (in kilodaltons) are indicated on the left. WT, wild type.

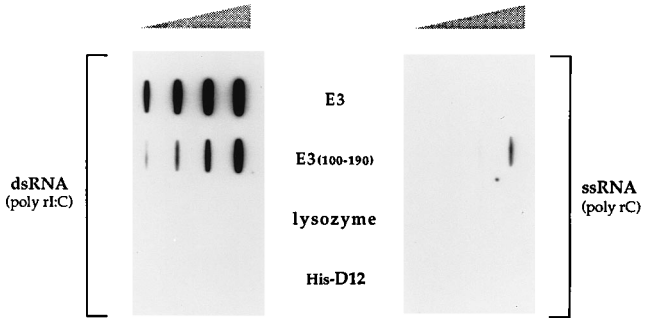

FIG. 3. Northwestern blot assay of RNA binding. Serial dilutions of each protein preparation (containing 63, 125, 250, and 500 ng of protein in 5 μl of buffer B) were applied to nitrocellulose membranes (0.2-μm-pore size [Bio-Rad]) with a Bio-Dot SF microfiltration apparatus. The membranes were preincubated in 15 ml of binding buffer (10 mM Tris HCl [pH 8.0], 1 mM EDTA, 50 mM NaCl, 0.04% bovine serum albumin [BSA], 0.04% Ficoll 400, 0.04% polyvinylpyrrolidone-40) for 30 min at room temperature with constant rocking motion. (BSA was included to block nonspecific binding of RNA to the membrane). The buffer was then decanted, and one membrane was overlaid with 15 ml of binding buffer containing ^{32}P-labeled poly(rC)-poly(rI) (7.5×10^5 Cerenkov cpm), while the other was probed with binding buffer containing ^{32}P-labeled poly(rC) (7.5×10^5 Cerenkov cpm). After incubation for 2 h at room temperature, the buffer containing the labeled RNA was removed and the membranes were washed three times with 15 ml of binding buffer (10 min of incubation per wash). The two membranes were air dried and exposed simultaneously to X-ray film for autoradiography.

His-tagged version of the 33-kDa vaccinia virus capping enzyme subunit D12 (14) was also unable to bind RNA; hence, the His tag did not account for RNA binding by E3(100–190).

To optimize the Northwestern blot assay for detection of mutational effects on dsRNA binding, we initially compared dsRNA binding by wild-type E3(100–190) with that of mutant E3(100–190)-K167A. Chang and Jacobs reported previously that mutating Lys-167 to Thr eliminated E3 binding to poly(rI)-poly(rC) agarose (4); hence, we had a high index of suspicion that the K167A mutant would be defective. To screen for conditions that would most clearly discriminate between active and presumptively inactive forms of E3(100–190), we varied the ionic strength of the binding buffer and tested the extent of RNA bound by serial dilutions of protein applied to the membrane (Fig. 4). dsRNA binding by full-length E3 was proportional to the amount of protein applied; the binding curves were essentially the same at 50, 125, 250, and 500 mM NaCl (Fig. 4, left panel). Wild-type E3(100–190) bound approximately fourfold less poly(rI)-poly(rC) per nanogram than did full-sized E3. E3(100–190) was also more sensitive to ionic strength; the binding curves shifted only slightly at 125 and 250 mM NaCl, but fell off more sharply at 0.5 M NaCl (Fig. 4, middle panel). The mutant protein E3(100–190)-K167A bound dsRNA weakly at 50 mM NaCl and precipitously lost affinity for dsRNA at higher salt concentrations (Fig. 4, right panel).

For the purpose of characterizing the entire collection of mutants in the dsRBM, we measured dsRNA binding at 250 mM NaCl. The extent of dsRNA binding was determined as a function of input protein. The titration curves shown in Fig. 5 are the average of three independent experiments. In each experiment, all 14 proteins were simultaneously titrated on the same membrane. The amount of labeled poly(rI)-poly(rC) bound by 250 ng of the wild-type E3(100–190) was defined as an arbitrary unit of 1.0, against which all other values were normalized. (The curves are displayed on three separate plots merely for the sake of clarity.) A 50% decrement in the dsRNA binding affinity was used as a threshold of significance in evaluating mutational effects. By this criterion, Ala substitutions at

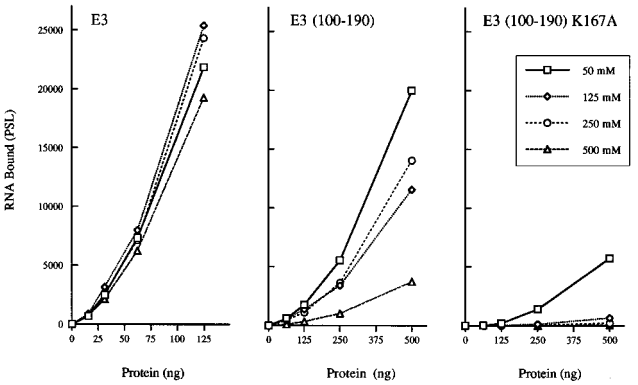

FIG. 4. Effect of NaCl on RNA binding. Serial dilutions of full-length recombinant E3 protein (11), the C-terminal RNA binding domain E3(100–190), and mutant E3(100–190)-K167A protein were applied to four nitrocellulose membranes, which were then preincubated in binding buffer containing either 50, 125, 250, or 500 mM NaCl. The membranes were probed with radiolabeled poly(rI)-poly(rC) in binding buffer at the same salt concentrations present during the preincubation. RNA bound in each slot was quantitated with a Fuji BAS1000 PhosphorImager; all four membranes were scanned simultaneously. The PhosphorImager signal (photo-stimulatable luminescence [PSL]) is plotted as a function of the amount (nanograms) of protein applied to the membrane. Titration curves for the full-length E3, wild-type E3(100–190), panel), and mutant E3(100–190)-K167A proteins are shown for each of the four NaCl concentrations (with symbols as indicated in the right panel).

6 of 14 residues were detrimental. The E124A, F148A, and K167A mutations were the most severe, reducing RNA binding to 2% of that of the wild type. The F135A, R168A, and K171A mutations reduced binding to 20 to 25% of that of the wild type. The remaining eight Ala substitutions did not cause significant loss of function. It is interesting to note that three of the mutants—N172A, N173A, and K176A—bound dsRNA slightly better than wild-type E3(100–190) at every level of input protein tested.

Genetic assay of E3(100–190) function in vivo. Expression of the C-terminal domain of E3 was toxic to *E. coli*; i.e., we could not recover ampicillin-resistant transformants when the T7-based E3(100–190) expression plasmid was introduced into *E. coli* BL21(DE3), a strain that carries the T7 RNA polymerase gene under control of a leaky *lac* promoter. The same plasmid readily transformed *E. coli* BL21, the parent strain lacking the T7 RNA polymerase gene. The tightness of the toxicity phenotype of the wild-type pET-E3(100–190) plasmid was reflected in the ratio of transformation efficiencies in BL21(DE3) versus BL21 (R), which was 9×10^{-5} (Table 1). In contrast, the pET14 vector transformed the two strains with nearly equivalent efficiencies (R = 0.46). The finding that the toxicity of E3(100–190) was completely eliminated by the K167A mutation (R = 0.45) argued that the lethal phenotype was dependent on the ability of the E3(100–190) protein to bind to dsRNA.

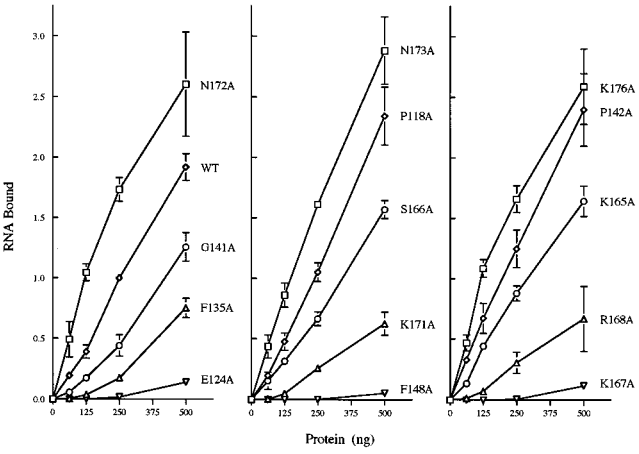

FIG. 5. Effect of alanine-substitution mutations on dsRNA binding by E3(100–190). Serial dilutions of the wild-type (WT) and mutated E3(100–190) proteins were applied to a nitrocellulose membrane, which was then preincubated in binding buffer containing 250 mM NaCl and subsequently probed with radiolabeled poly(rI)-poly(rC). RNA bound in each slot was quantitated with a PhosphorImager. The PhosphorImager signal intensity was plotted as a function of the amount (nanograms) of each protein applied to the membrane. The data shown represent the average of three separate experiments; for each experiment, the amount of RNA bound by 250 ng of wild-type E3(100–190) was assigned an arbitrary value of 1.0, against which all other values were normalized. Standard error bars are included for each datum point.

TABLE 1. Efficiency of transformation of *E. coli* BL21(DE3) by pET-E3(100–190) plasmids

Plasmid	Transformation efficiency[a]		Ratio of BL21(DE3) to BL21[b]
	BL21(DE3)	BL21	
pET14b	1.2×10^6	2.6×10^6	0.46
pET-E3(100–190)	2.7×10^2	3.0×10^6	9.0×10^{-5}
P118A	4.0×10^2	1.2×10^6	3.3×10^{-4}
E124A	1.8×10^5	1.1×10^6	0.16
F135A	9.6×10^4	3.2×10^6	3.0×10^{-2}
G141A	2.0×10^2	8.2×10^5	2.4×10^{-4}
P142A	9.0×10^2	2.8×10^6	3.2×10^{-4}
F148A	5.0×10^5	2.5×10^6	0.20
K165A	4.9×10^3	5.4×10^6	9.1×10^{-4}
S166A	9.7×10^4	1.9×10^6	5.1×10^{-2}
K167A	1.3×10^6	2.9×10^6	0.45
R168A	1.8×10^5	1.9×10^6	9.5×10^{-2}
K171A	2.2×10^5	2.7×10^6	8.1×10^{-2}
N172A	3.0×10^2	1.9×10^6	1.6×10^{-4}
N173A	9.0×10^2	3.4×10^6	2.6×10^{-4}
K176A	6.0×10^2	2.7×10^6	2.2×10^{-4}

[a] *E. coli* BL21 and BL21(DE3) were transformed with serial dilutions of each plasmid (1, 10, and 100 ng of DNA per transformation). Colonies were counted 14 h after plating of the transformed cells on Luria-Bertani agar plates containing 0.1 mg of ampicillin per ml. The transformation efficiencies are expressed as the number of ampicillin-resistant colonies per microgram of plasmid DNA.
[b] R in text.

This conclusion was reinforced by transformation tests of the full collection of Ala-substitution mutants (Table 1). Mutants that retained full ability to bind dsRNA in vitro (P118A, G141A, P142A, K165A, N172A, N173A, and K176A) were toxic to BL21(DE3). Those mutations that inactivated dsRNA binding in vitro (E124A, F148A, and K167A) were well tolerated by BL21(DE3) (R = 0.16 to 0.45). Mutations that partially inactivated dsRNA binding in vitro (F135A, R168A, and K171A) increased specific transformation efficiency by 300- to 1,000-fold over wild-type E3(100–190). These mutant proteins still had some effect on bacterial growth insofar as the colony size of the transformants was smaller than that seen for pET14b (not shown). A similar loss of toxicity was seen with S166A, a mutant which did not appear to affect dsRNA binding in vitro. It is possible that the S166A mutation alleviated toxicity by an alternative mechanism, perhaps by lowering the level of the E3(100–190) protein in BL21(DE3). This case excepted, there was a fairly strong correlation between in vivo toxicity of mutant E3(100–190) alleles and in vitro dsRNA binding by purified E3(100–190) mutant proteins. This phenotype for loss of E3 function should prove useful in selecting for binding-defective mutants from pools of randomly mutated

E3(100–190) genes, as has been described for other gene products whose expression is toxic to *E. coli* BL21(DE3) (18).

Residues important for dsRNA binding are situated on the same face of the dsRBM. Alanine substitutions at 6 of 14 positions targeted in the E3 dsRBM caused significant reductions in dsRNA binding in vitro and alleviated the toxicity of E3(100–190) expression in bacteria. These six residues—Glu-124, Phe-135, Phe-148, Lys-167, Arg-168, and Lys-171—are conserved in dsRBMs found in dsRAD, staufen, and RNase III (Fig. 1) as well as many other members of the dsRBM protein family (1, 12, 19). However, sequence conservation is not a guarantor of functional relevance, insofar as three of the positions at which Ala substitution was tolerated—Pro-118, Gly-141, and Pro-142—are well conserved in other dsRBMs and have generally been regarded as part of the consensus sequence that defines this motif (1, 12, 19).

Our mutational findings are in accord with those reported for other dsRBMs. For example, alanine substitutions in the staufen-3 dsRBM at Phe-32 (equivalent to Phe-148 of E3), and basic residues Lys-50, Lys-51, and Lys-54 (the analogs of E3 positions Lys-167, Arg-168, and Lys-171) reduced or eliminated dsRNA binding when the mutated dsRBMs were expressed as glutathione *S*-transferase fusion proteins in bacteria (3). Mutations in equivalent residues in the PKR-1 dsRBM also reduced or abolished dsRNA binding (9, 10, 16).

These mutational effects on E3 function, while informative per se, are particularly relevant in the context of the nuclear magnetic resonance structures recently reported for the staufen and RNase III dsRNA binding domains (3, 12). Both structures adopt an α-β-β-β-α topology in which the two α-helices lie on the same side of a three-stranded antiparallel β-sheet. The amino acid residues that compose the α-helices and β-strands are denoted below the sequences of the staufen and RNase III dsRBMs in Fig. 1. The three basic residues important for E3 dsRNA binding, which are conserved in staufen and RNase III, map to the proximal end of the second α-helix and to the loop connecting the helix to the third β-strand. The basic side chains are oriented toward the solvent-exposed face on a space-filling model of the staufen dsRBM. The critical residue Phe-148 is situated within the second β-strand, with the aromatic side chain partially exposed on the protein surface, close to Lys-167. Essential residue Glu-124 is located within the first α-helix, with its side chain exposed on the same face of the staufen dsRBM as those of the other residues found by mutagenesis to be relevant to dsRNA binding. On the basis of the nuclear magnetic resonance structures and mutational effects, it has been suggested that the loop/helix-2 region containing key basic residues makes direct contact with dsRNA (3, 12). The present data suggest that the first α-helix (containing an essential Glu) may participate in ligand binding.

This work was supported by grant GM42498 from the National Institutes of Health.

REFERENCES

1. **Bass, B. L., S. R. Hurst, and J. D. Singer.** 1994. Binding properties of newly identified Xenopus proteins containing dsRNA-binding motifs. Curr. Biol. **4:** 301–314.
2. **Beattie, E., E. Paoletti, and J. Tartaglia.** 1995. Distinct patterns of IFN sensitivity observed in cells infected with vaccinia K3L− and E3L− mutant viruses. Virology **210:**254–263.
3. **Bycroft, M., S. Grunert, A. G. Murzin, M. Proctor, and D. St. Johnston.** 1995. NMR solution structure of a double-stranded RNA-binding domain from Drosophila stuafen protein reveals homology to the N-terminal domain of ribosomal protein S5. EMBO J. **14:**3563–3571.
4. **Chang, H.-W., and B. L. Jacobs.** 1993. Identification of a conserved motif that is necessary for binding of the vaccinia virus E3L gene products to double-stranded RNA. Virology **194:**537–547.
5. **Chang, H.-W., L. H. Uribe, and B. L. Jacobs.** 1995. Rescue of vaccinia virus lacking the E3L gene by mutants of E3L. J. Virol. **69:**6605–6608.
6. **Chang, H.-W., J. C. Watson, and B. L. Jacobs.** 1992. The E3L gene of vaccinia virus encodes an inhibitor of the interferon-induced, double-stranded RNA-dependent protein kinase. Proc. Natl. Acad. Sci. USA **89:** 4825–4829.
7. **England, T. E., and O. C. Uhlenbeck.** 1978. 3′-terminal labelling of RNA with T4 RNA ligase. Nature (London) **275:**560–561.
8. **Gatignol, A., A. Buckler-White, B. Berkhout, and K. T. Jeang.** 1991. Characterization of a human TAR RNA-binding protein that activates the HIV-1 LTR. Science **251:**1597–1600.
9. **Green, S. R., L. Manche, and M. B. Mathews.** 1995. Two functionally distinct RNA-binding motifs in the regulatory domain of the protein kinase DAI. Mol. Cell. Biol. **15:**358–364.
10. **Green, S. R., and M. B. Mathews.** 1992. Two RNA-binding motifs in the double-stranded RNA-activated protein kinase, DAI. Genes Dev. **6:**2478–2490.
11. **Ho, C. K., and S. Shuman.** Physical and functional characterization of the double-stranded RNA binding protein encoded by the vaccinia virus E3 gene. Virology, in press.
12. **Kharrat, A., M. J. Macias, T. J. Gibson, M. Nilges, and A. Pastore.** 1995. Structure of the dsRNA binding domain of *E. coli* RNase III. EMBO J. **14:** 3572–3584.
13. **Kim, U., Y. Wang, T. Sanford, Y. Zeng, and K. Nishikura.** 1994. Molecular cloning of cDNA for double-stranded RNA adenosine deaminase, a candidate enzyme for nuclear RNA editing. Proc. Natl. Acad. Sci. USA **91:** 11457–11461.
14. **Mao, X., and S. Shuman.** 1994. Intrinsic RNA (guanine-7) methyltransferase activity of the vaccinia virus capping enzyme D1 subunit is stimulated by the D12 subunit. Identification of amino acid residues in the D1 protein required for subunit association and methyl group transfer. J. Biol. Chem. **269:**24472–24479.
15. **McCormack, S. J., D. C. Thomis, and C. E. Samuel.** 1992. Mechanism of interferon action: identification of a RNA binding binding domain within the N-terminal region of the human RNA-dependent P1/eIF2 alpha protein kinase. Virology **188:**47–56.
16. **McMillan, N. A. J., B. W. Carpick, B. Hollis, W. M. Toone, M. Zamanian-Daryoush, and B. R. G. Williams.** 1995. Mutational analysis of the double-stranded RNA (dsRNA) binding domain of the dsRNA-activated protein kinase, PKR. J. Biol. Chem. **270:**2601–2606.
17. **Miller, J. E., and C. E. Samuel.** 1992. Proteolytic cleavage of the reovirus sigma 3 protein results in enhanced double-stranded RNA-binding activity: identification of a repeated basic amino acid motif within the C-terminal binding region. J. Virol. **66:**5347–5356.
18. **Morham, S. G., and S. Shuman.** 1990. Phenotypic selection and characterization of mutant alleles of a eukaryotic DNA topoisomerase I. Genes Dev. **4:**515–524.
19. **St. Johnston, D., N. H. Brown, J. G. Gall, and M. Jantsch.** 1992. A conserved double-stranded RNA-binding domain. Proc. Natl. Acad. Sci. USA **89:** 10979–10983.
20. **Studier, F. W., A. H. Rosenberg, J. J. Dunn, and J. W. Dubendorff.** 1990. Use of T7 RNA polymerase to direct expression of cloned genes. Methods Enzymol. **185:**60–89.
21. **Watson, J. C., H. W. Chang, and B. L. Jacobs.** 1991. Characterization of a vaccinia virus-encoded double-stranded RNA-binding protein that may be involved in inhibition of the double-stranded RNA-dependent kinase. Virology **185:**206–216.
22. **Yuwen, H., J. H. Cox, J. W. Yewdell, J. R. Bennink, and B. Moss.** 1993. Nuclear localization of a double-stranded RNA-binding protein encoded by the vaccinia virus E3L gene. Virology **195:**732–744.